

Elastic Buckling Loads of Cold-Formed Steel Channel Sections with Perforations



Ngoc Hieu Pham*

Department of Civil Engineering, Hanoi Architectural University, Vietnam

Submission: January 23, 2022; **Published:** April 13, 2022

***Corresponding author:** Ngoc Hieu Pham, Department of Civil Engineering, Hanoi Architectural University, Vietnam

Abstract

Cold-formed perforated steel sections have been commonly applied to meet the demands for technical installations, leading to the reduction of capacities of these such sections. The capacities of these sectional types have been considered in the American Specification AISI S100-16 using the Direct Strength Method (DSM). This method known as the innovative method for the design of cold-formed steel sections allows predicting the sectional capacities of perforated sections based on elastic buckling loads. Elastic buckling analyses are compulsory for the application of the DSM in the design. The determination of elastic buckling loads of perforated sections is cumbersome with the usage of current buckling analysis software programs. The paper, therefore, presents a simple method for the determination of elastic buckling loads of cold-formed perforated channel sections, especially the paper is aimed to introduce a module software program used for elastic buckling analyses of these such channel sections based on this simple method. This program is convenient for buckling analysis, and it becomes a key program for the application of DSM in the design of cold-formed perforated steel channel sections. This software program is subsequently utilized to investigate the effects of web hole dimensions on the elastic buckling loads of cold-formed steel channel sections with perforations under compression or bending. The investigated results provide fundamental understandings of the buckling behaviors of perforated channel sections due to the effects of the web holes.

Keywords: Elastic buckling loads; Cold-formed steel channel sections; Perforations; Compression; Bending

Introduction

Cold-formed steel sections with perforations have been found in structural applications due to the demand for the installations of electrical, plumbing or heating services. The holes are commonly pre-punched in the web of channel or Zed sections; this affects the elastic buckling loads and the capacities of these such sections. Their sectional capacities are determined as regulated in the American Specification AISI S100 [1] with the application of the Direct Strength Method (DSM). This method has been illustrated its advantages in the design of cold-formed steel structures compared to the effective width method (EWM) [2] due to its simplicity and effectiveness in the design. This method can predict the strengths of cold-formed steel sections or members on the basis of elastic buckling loads. Therefore, the determination of these elastic buckling loads is the key step for the application of the DSM in the design of cold-formed steel sections.

The elastic buckling analysis for cold-formed steel sections without holes can be determined from an elastic buckling

curve or a "signature curve" obtained by using THIN-WALL-2 or CUFISM software programs [3,4]. These software programs were developed based on the finite strip method [5]. The elastic buckling analyses of cold-formed steel channel sections without holes were presented in Pham & Vu [6] with the application of the THIN-WALL-2 software program [3]. These buckling analysis programs, however, cannot be used for these perforated sections due to the discontinuities of these strips in such sections caused by the presence of holes. Finite element models can be used in these cases with the applications of popular software programs such as ANSYS or ABAQUS [7]. FE models are found to be computationally inefficient, subjective and laborious in the buckling analysis. A large number of buckling modes obtained in the analysis must be visually inspected to identify whether the modes are local or distortional buckling's, even cannot be identified due to the interaction between modes.

In the literature, cold-formed stub columns with the variation of hole shapes were investigated to study the local buckling

strengths [8-11]. The hole lengths or locations were considered to study the hole impacts on the capacities of cold-formed steel columns [12-15]. The strength and behavior of cold-formed steel channel sections with perforations were studied by Moen & Schafer [16-23], which are subsequently introduced in the American Specification AISI S100-16 [1] for the design of these such sections using the Direct Strength Method (DSM). In their studies, a new simplified method was developed to determine elastic buckling loads of cold-formed perforated steel sections, which was a key step for the application of DSM in the design of cold-formed steel channel sections with perforations, as regulated in AISI S100-16 [1]. Recently, a module CUFSM software program developed by The American Iron and Steel Institute [24] based on research results of Moen & Schafer [16-23], allows the designer to simply determine the elastic buckling loads of these such sections.

The paper, therefore, presents the alternative approach to determine the elastic buckling loads of cold-formed perforated steel channel sections instead of using finite element buckling analyses. Based on the alternative method, the module CUFSM software program will be introduced for elastic buckling analyses of the perforated channel sections that can be used for the design of the cold-formed steel channel sections with perforations using DSM. This buckling analysis program is subsequently used to investigate the effects of web hole dimensions on the elastic buckling loads of cold-formed steel channel sections with perforations, which allows understanding the buckling behaviors of cold-formed steel channel sections with perforations.

Simplified Method for the Determination of Elastic Buckling Loads of Cold-Formed Perforated Steel Sections

The simplified method is applied for the buckling analysis of cold-formed steel sections with perforations, as presented in Moen & Schafer [16-18] or in Appendix 2, AISI S100-16 [1]. The elastic local buckling loads ($P_{cri}; M_{cri}$) for cold-formed steel sections with holes under compression or bending are determined as follows:

$$P_{crl} = \text{Min}(P_{crlnh}; P_{crlh}) \quad (1)$$

$$M_{crl} = \text{Min}(M_{crlnh}; M_{crlh}) \quad (2)$$

where ($P_{crlnh}; M_{crlnh}$) are the local buckling loads of the gross cross-sections which can be determined using finite strip methods such as THIN-WALL-2 or CUFSM software programs [3,4]; ($P_{crlh}; M_{crlh}$) are the buckling loads of net cross-sections and are also calculated by using finite strip analyses. Elastic buckling analyses are carried out for the net cross-sections to get the elastic buckling curves, as illustrated in Figure 1, where L_{crlh} is the half-wavelength corresponding to the critical buckling load. The hole length is considered in this analysis as follows: the buckling loads ($P_{crlh}; M_{crlh}$) are equal to the critical buckling loads if $L_{hole} > L_{crlh}$ (Figure 1a) and are equal to the buckling loads at the lengths of holes if $L_{hole} < L_{crlh}$ (Figure 1b).

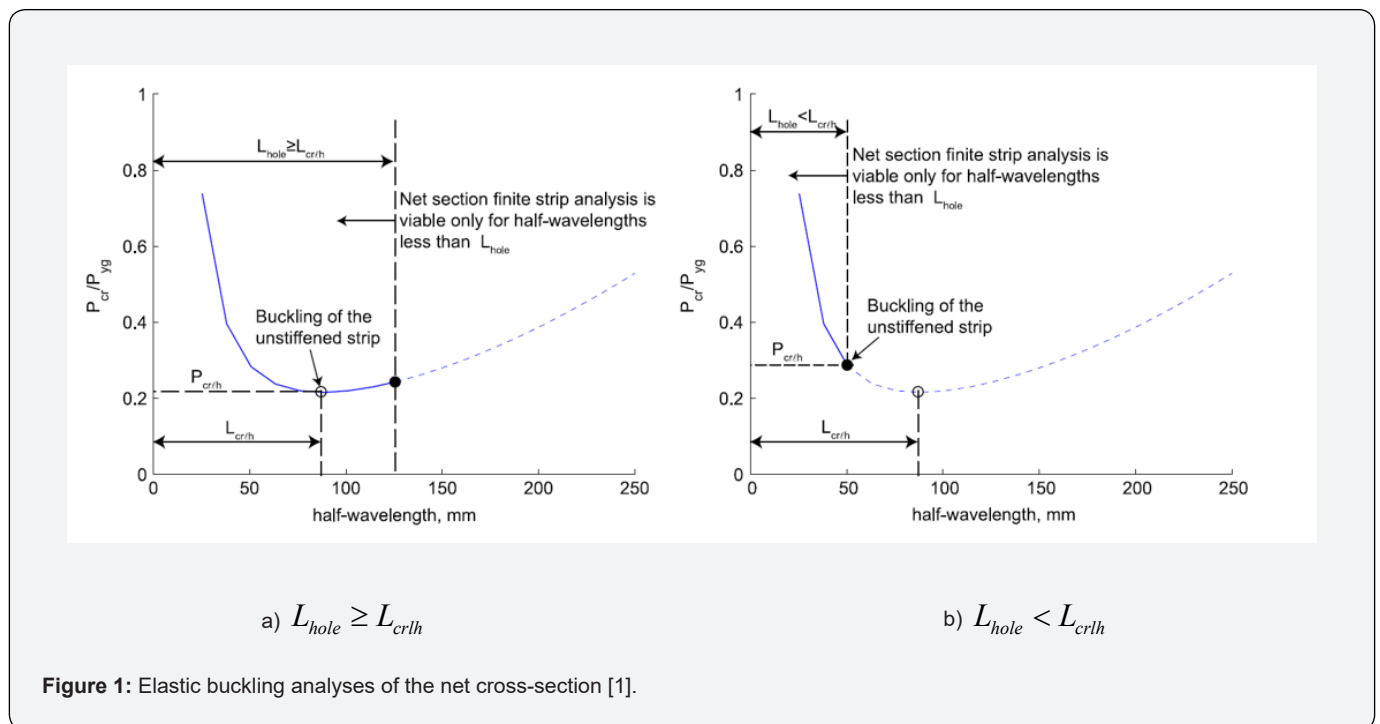


Figure 1: Elastic buckling analyses of the net cross-section [1].

The distortional buckling loads (P_{crd} , M_{crd}) are determined using the approximate method as follows: Elastic buckling analyses of the gross cross-sections are implemented to identify the half-wavelengths (L_{crd}) of distortional buckling's. The web thickness (t) is subsequently converted into the assumed thickness (t_r) to consider the effects of the web holes, as demonstrated in Equation (3), where L_h is the hole length. The distortional buckling loads (P_{crd} ; M_{crd}) are determined based on elastic buckling analyses of the modified cross-sections.

$$t_r = t \left(1 - \frac{L_h}{L_{crd}} \right)^{1/3} \quad (3)$$

To support these buckling analyses, a module CUFSM software program developed by The American Iron and Steel Institute allows considering the effects of the web holes on the elastic buckling loads, as fully reported in [24]. This program requires simple inputs and directly provides the elastic buckling analyses of both cross-sections with and without holes, as illustrated in (Figure 2). This program will be used to investigate the effects of the web hole dimensions of the elastic buckling loads of cold-formed steel channel sections with perforations in this study.

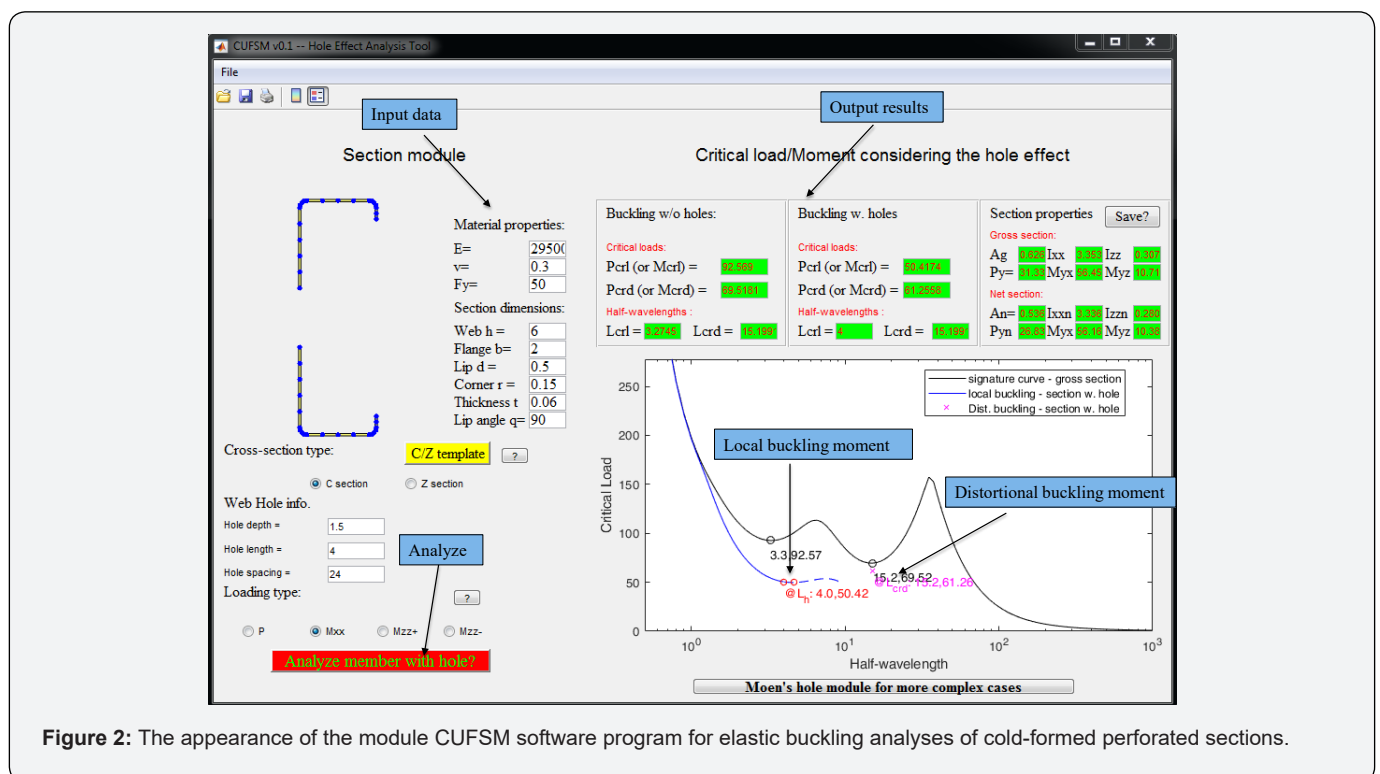


Figure 2: The appearance of the module CUFSM software program for elastic buckling analyses of cold-formed perforated sections.

Impacts of Web Hole Dimensions on the Elastic Buckling Loads of Cold-formed Perforated Steel Channel Sections under Compression or Bending

Based on Pham's report [25] and the simple method presented in the previous section. it was found that the local buckling loads only depend on the ratios of the web hole heights and the sectional depths (h_{hole}/D), whereas they are the ratios between the hole lengths and the sectional depths (L_{hole}/D) for distortional buckling. Therefore, the effects of hole dimension components on the elastic buckling loads are separately considered in the investigation. The channel sections for the investigation are listed in Table 1 with the nomenclature illustrated in Figure 3.

Table 1: The dimensions of channel sections (Unit: mm).

Sections	t	D	B	L
C15012	1.2	152	64	14.5
C20015	1.5	203	76	19.5
C25019	1.9	254	76	21.5
C30024	2.4	300	96	27.5
C35030	3	350	125	30
C40030	3	400	125	30

Note: Inner radius r = 5mm.

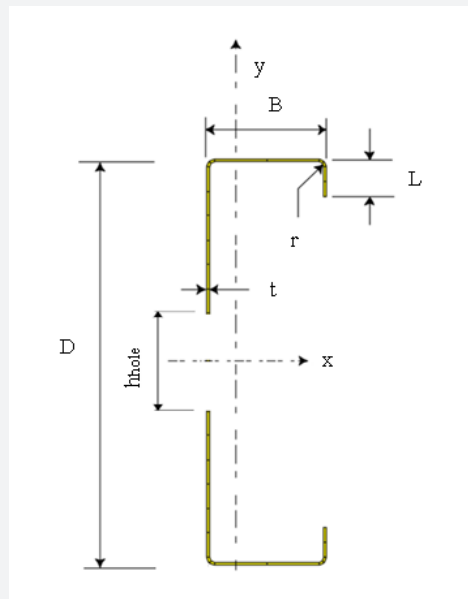


Figure 3: Nomenclature of perforated channel sections.

The web hole heights & elastic local buckling loads

The ratios h_{hole}/D are taken from 0.05 to 0.8. The hole lengths L_{hole} are selected as two times of the sectional depths (D) to ensure these lengths are larger than the half-wavelengths L_{hole} of critical local buckling loads of the net cross-sections ($L_{hole} > L_{cr,h}$). The elastic local buckling loads of the net cross-sections are illustrated in Figures 4 & 5 in comparison with those of the gross cross-sections.

The investigated results show that the local buckling loads are seen as upward trends if the hole lengths increase. The local buckling's are occurred at the net cross-section for small hole heights, whereas these buckling's are obtained at the flat web areas between holes for the large ones. The local buckling loads of the net cross-sections with small hole heights are less than those of the gross cross-sections, this results in the occurrence of local buckling's at the net cross-sections. In terms of large hole heights, the buckling loads of the net cross-sections are found to be larger than those of the gross cross-sections; the occurrence of local buckling's, therefore, are at the flat web areas between holes. This is explained that if the hole heights increase, the flat areas above and under the holes in the web become smaller leading to the reductions of the slenderness of these areas and the increase of the web hole stability.

For compression, when the ratios h_{hole}/D reach 0.22 for all investigated sections, the local buckling loads of the gross and net cross-sections become equal. The elastic local buckling loads of

perforated steel channel sections ($P_{cr,t}$), therefore, can be taken as these buckling loads of the gross cross-sections if the ratios h_{hole}/D are higher than 0.22. Also, Figure 4 shows that the curves of ratios ($P_{cr,h}/P_{cr,ln,h}$) are nearly unchanged with the variations of the investigated channel sections when the ratios (h_{hole}/D) are less than 0.22. It means that the elastic local buckling load of a perforated channel cross-section can be determined based on the ratios ($P_{cr,h}/P_{cr,ln,h}$) in Figure 4 and the local buckling loads of the gross cross-sections ($P_{cr,ln,h}$). For bending, the effects of web holes on the elastic local buckling moments are significant with the reductions reaching 40% compared to those of the gross cross-sections. Local buckling can be occurred at the net cross-section if the ratios (h_{hole}/D) are less than 0.6, even 0.8 for C15012 section. Similar to compression, the curves of ratios ($M_{cr,h}/M_{cr,ln,h}$) are quite stable for the investigated cross-sections when the ratios h_{hole}/D are less than 0.6. Also, the local buckling's are occurred at the net cross-sections if the ratios h_{hole}/D are less than about 0.65. Therefore, if the ratios h_{hole}/D are more than about 0.65, the elastic local buckling moments of the perforated channel sections ($M_{cr,t}$) can be taken as those of gross cross-sections ($M_{cr,ln,h}$), except C15012, and; the local buckling's will be occurred at the flat web areas between holes (Figure 5).

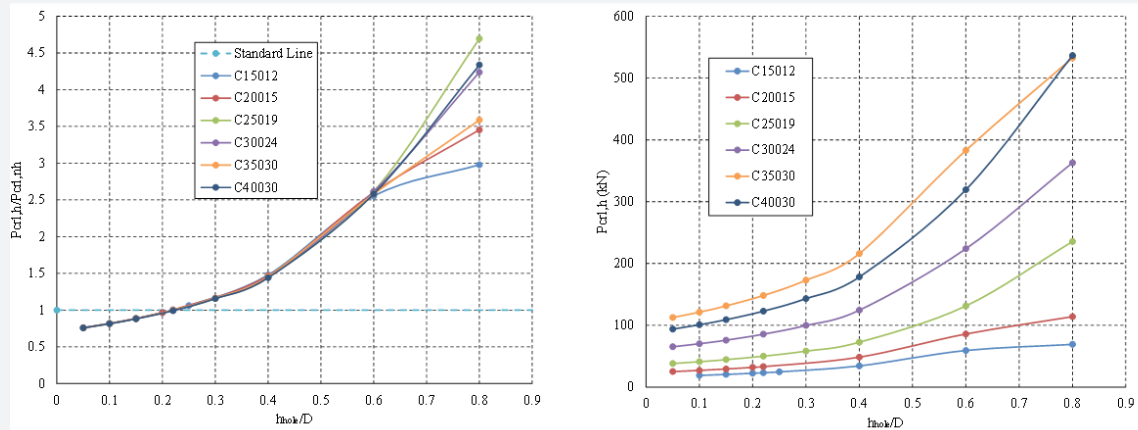


Figure 4: Elastic local buckling loads under compression.
 Note: $P_{cr,lnk}$ and $P_{cr,lnh}$ are the elastic local buckling loads of the gross and net cross-sections.

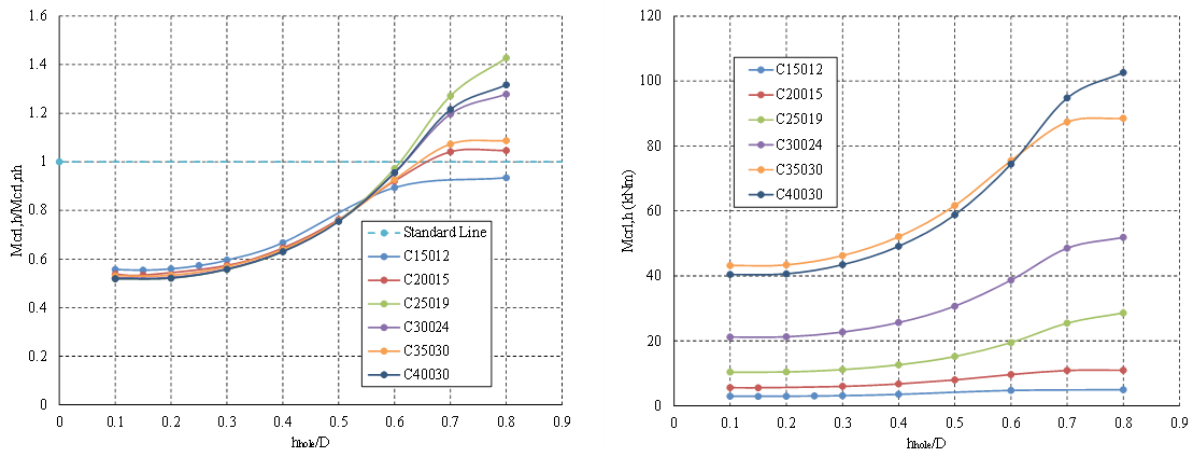


Figure 5: Elastic local buckling loads under bending.
 Note: $M_{cr,lnk}$ and $M_{cr,lnh}$ are the elastic local buckling moments of the gross and net cross-sections.

The web hole lengths & elastic distortional buckling loads

The ratios of the web hole lengths and the sectional depths L_{hole}/D are taken from 0.5 to 3.0 and the hole heights (h_{hole}) are taken as half of the sectional depths (D). The effects of the web hole dimensions on the elastic distortional buckling loads are carried out with the investigated sections listed in Table 1. The investigated results are illustrated in Figures 6 & 7 for the comparisons of the elastic distortional buckling loads between the perforated cross-sections and the gross cross-sections.

Based on the investigated results, it is found that the elastic distortional buckling loads are seen as downward trends when the ratios (L_{hole}/D) increase. Also, it was found that if the ratios of

the web depths and the flange widths (W/F) increase, the effects of the web hole lengths on the elastic distortional buckling loads become clearer. This can be illustrated as follows: the ratio (W/F) of C15012 section is 2.38, then the reductions of elastic distortional buckling loads are about 40% for both compression or bending; whereas these reductions are about 65% when the ratio (W/F) is 3.23 for C40030 section. This can be explained due to the influence of web depths on the distortional buckling behaviors of the flange. The webs with high stability (it means the ratio (W/F) is small) allow to reduce the effects of the web holes on the distortional buckling of the flanges, and vice versa. Evenly, the high web slenderness of C40030 sections leads to its elastic distortional buckling loads becoming less than those of C35030 section under compression, as illustrated in Figure 6.

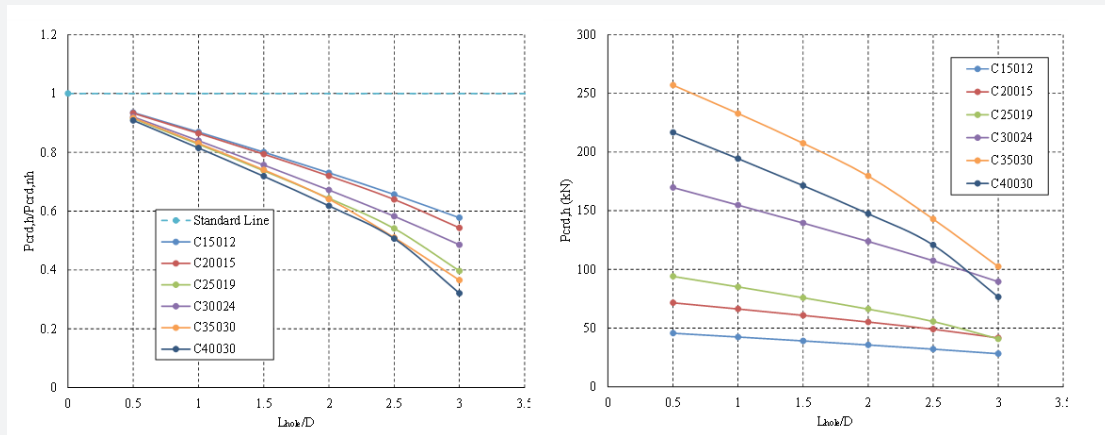


Figure 6: Elastic distortional buckling loads under compression.
 Note: $P_{cr,dh}$ and $P_{cr,n,h}$ are the elastic distortional buckling loads of the net and gross cross-sections.

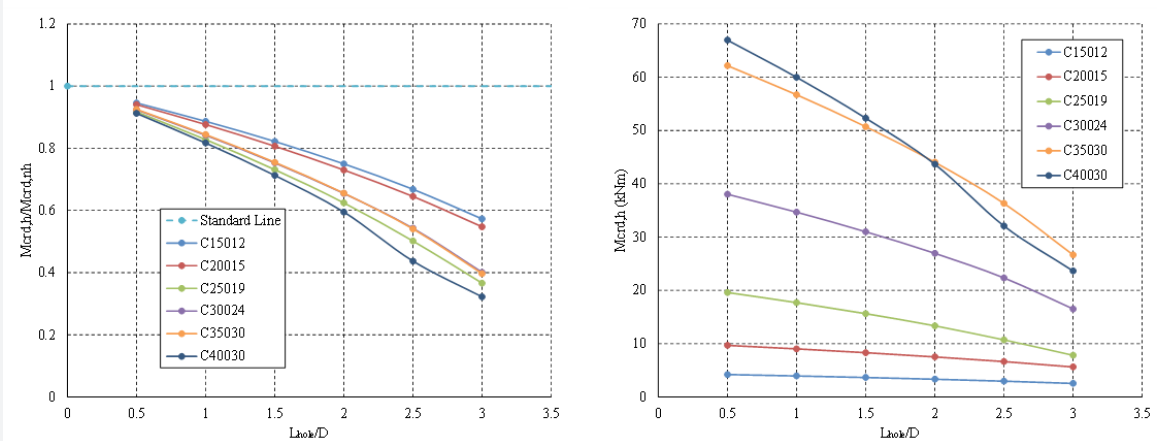


Figure 7: Elastic distortional buckling loads under bending.
 Note: $M_{cr,dh}$ and $M_{cr,n,h}$ are the elastic distortional buckling moments of the net and gross cross-sections.

Conclusion

This paper presents the simple method in the determination of elastic buckling loads of cold-formed steel sections with perforations according to American Specification AISI S100-16. This method is the base for the recent development of the module CUFSM software program by The American Iron and Steel Institute to support the buckling analyses of cold-formed perforated steel channel sections. The paper is aimed to introduce this module program for the designers in the buckling analysis and then utilize this program to investigate the effects of the web hole dimensions on the elastic buckling loads of cold-formed steel channel sections with perforations. The following conclusions are provided based on the investigated results, as follows:

- a. Elastic local buckling loads are significantly affected by the web hole heights, whereas the web hole lengths are noticeable impacts on the elastic distortional buckling loads.
- b. The elastic local buckling loads are seen as upward trends if the hole heights increase. Local bucklings intend to occur at the holes when the web hole heights are small but occur between holes for large hole heights.
- c. When the hole lengths increase, the distortional buckling loads undergo downward trends. The ratios W/F increase, the effects of the web holes on the elastic distortional buckling loads become more noticeable.

These remarks provide fundamental understandings of elastic buckling behaviors of cold-formed steel channel sections with perforations.

References

1. American Iron and Steel Institute (2016) North American Specification for the Design of Cold-formed Steel Structural Members. Washington DC: American Iron and Steel Institute.
2. Schafer BW, Peköz T (1998) Direct Strength Prediction of Cold-Formed Members Using Numerical Elastic Buckling Solutions. Fourteenth International Specialty Conference on Cold-Formed Steel Structures p: 1-8.
3. Nguyen VV, Hancock GJ, Pham CH (2015) Development of the Thin-Wall-2 for Buckling Analysis of Thin-Walled Sections Under Generalized Loading. Proceeding of 8th International Conference on Advances in Steel Structures.
4. Li Z, Schafer BW (2010) Buckling analysis of cold-formed steel members with general boundary conditions using CUFSM: Conventional and constrained finite strip methods. Saint Louis, Missouri, USA.
5. Cheung YK (1976) Finite strip method in structural analysis.
6. Pham NH, Vu QA (2021) Effects of stiffeners on the capacities of cold-formed steel channel members. Steel Construction 14(4): 270-278.
7. Dassault Systemes Simulia Corp (2014) ABAQUS/CAE User's Manual. Providence, RI, USA.
8. Ortiz-Colberg RA (1981) The load carrying capacity of perforated cold-formed steel columns. Cornell University, Ithaca, NY, USA.
9. Sivakumanran KS (1987) Load capacity of uniformly compressed cold-formed steel section with punched web. Can J Civil Eng 14(4): 8.
10. Banwait AS (1987) Axial load behaviour of thin-walled steel sections with openings. McMaster University, Hamilton, Ontario, Canada.
11. Abdel-Rahman N (1997) Cold-formed steel compression members with perforations. McMaster University, Hamilton, Ontario, Canada.
12. Rhodes J, Schneider FD (1994) The compressional behaviour of perforated elements. Twelfth international specialty conference on cold-formed steel structures p. 11-28.
13. Loov R (1984) Local buckling capacity of C-shaped cold-formed steel sections with punched webs. Can J Civil Eng 11(1): 1-7.
14. Pu Y, Godley MHR, Beale RG, Lau HH (1999) Prediction of ultimate capacity of perforated lipped channels. Journal of Structural Engineering 125(5): 510.
15. Rhodes J, Macdonald M (1996) The effects of perforation length on the behaviour of perforated elements in compression. Thirteenth international specialty conference on cold-formed steel structures pp. 91-101.
16. Moen CD (2008) Direct Strength design for cold-formed steel members with perforations. Johns Hopkins University, Baltimore, USA.
17. Moen CD, Schafer BW (2008) Experiments on cold-formed steel columns with holes. Thin-Walled Structures 46(10): 1164-1182.
18. Moen CD, Schafer BW (2009) Elastic buckling of cold-formed steel columns and beams with holes. Engineering Structures 31(12): 2812-2824.
19. Moen CD, Schafer BW (2006) Impact of holes on the elastic buckling of cold-formed steel columns. International Specialty Conference on Cold-Formed Steel Structures pp. 269-283.
20. Moen CD, Schafer BW (2010) Extending direct strength design to cold-formed steel beams with holes. 20th International Specialty Conference on Cold-Formed Steel Structures - Recent Research and Developments in Cold-Formed Steel Design and Construction 171-183.
21. Cai J, Moen CD (2016) Elastic buckling analysis of thin-walled structural members with rectangular holes using generalized beam theory. Thin-Walled Structures 107: 274-286.
22. Moen CD, Schafer BW (2009) Elastic buckling of thin plates with holes in compression or bending. Thin-Walled Structures 47(12): 1597-1607.
23. Moen CD, Schudlich A, Heyden A (2013) Experiments on Cold-Formed Steel C-Section Joists with Unstiffened Web Holes. Journal of Structural Engineering 139(5): 695-704.
24. American Iron and Steel Institute (2021), Development of CUFSM Hole Module and Design Tables for the Cold-formed Steel Cross-sections with Typical Web Holes in AISI D100. AISI D100, Research Report RP21-01.
25. Pham NH (2021) Investigation of web hole effects on the elastic buckling loads of cold-formed steel members. Research Report, Hanoi Architectural University, Vietnam.



This work is licensed under Creative Commons Attribution 4.0 License
DOI: [10.19080/CERJ.2022.13.555852](https://doi.org/10.19080/CERJ.2022.13.555852)

Your next submission with Juniper Publishers will reach you the below assets

- Quality Editorial service
- Swift Peer Review
- Reprints availability
- E-prints Service
- Manuscript Podcast for convenient understanding
- Global attainment for your research
- Manuscript accessibility in different formats
(Pdf, E-pub, Full Text, Audio)
- Unceasing customer service

Track the below URL for one-step submission

<https://juniperpublishers.com/online-submission.php>